Wide-Temperature-Range Kinetics of the Reactions of Cu with Cl_2 and N_2O and of CuCl with Cl_2

Biljana Cosic, David P. Belyung,† Jasmina Hranisavljevic,‡ and Arthur Fontijn*

High-Temperature Reaction-Kinetics Laboratory, Isermann Department of Chemical Engineering, Rensselaer Polytechnic Institute, Troy, New York 12180-3590

Received: April 28, 2003; In Final Form: August 14, 2003

The reactions Cu + Cl_2 → CuCl + Cl (1), CuCl + Cl_2 → $CuCl_2$ + Cl (2), and Cu + N_2O → CuO + N_2 (3) have been studied using a high-temperature fast-flow reactor (HTFFR). The metallic species were the limiting reactants. Cu atoms were generated by vaporization, and CuCl, by reaction 1. Their concentrations were monitored by LIF. The following $k(T)$ expressions in cm^3 $molecule^{-1}$ s^{-1} were obtained: $k_1(305-1140\ K) = 3.9 \times 10^{-10} \exp(-355\ K/T)$, $k_2(980-1150\ K) = 3.1 \times 10^{-11} \exp(-4765\ K/T)$, and $k_3(530-950\ K) = 3.8 \times 10^{-10} \exp(-5441\ K/T)$. The Arrhenius parameters of k_1 are similar to other exothermic metal atom−Cl_2 reactions. The activation energy of reaction 2 is rather large, which is attributed to the closed-shell electron structure of CuCl. Reaction 3 had been measured earlier in a pseudostatic photochemistry reactor (Narayan, A. S.; Futerko, P. M.; Fontijn, A. *J. Phys. Chem.* **1992**, *96*, 290) and in a different type of fast-flow reactor (Vinckier, C.; Verhaeghe, T.; Vanhees, I. *J. Chem. Soc., Faraday Trans.* **1994**, *90*, 2003). A comparison of these two studies showed mild disagreement. However, a critical evaluation of the three data sets confirms the validity of our previous recommendation: $k_3(470-1340\ K) = 3.04 \times 10^{-20}(T/K)^{2.97} \exp(-3087\ K/T)$.

Introduction

Studies using model fly ash have suggested that $CuCl_2$ is the most efficient catalyst in the formation of highly toxic polychlorinated dioxins and dibenzofurans in the cooler zones of waste incinerators.[1] Such studies, done to determine the catalytic mechanisms involved, suggest that the role of $CuCl_2$ is complex.[1−6] It acts as a chlorinating agent of small hydrocarbons and further catalyzes their condensation to higher, aromatic products.[6] $CuCl_2$ is also known to chlorinate particulate carbonaceous matter and its subsequent oxidative degradation catalytically.[3] Recent studies indicate that during chlorination Cu^{2+} is reduced to Cu^+. The catalytic activity directly depends on the ability to regenerate, that is, reoxidize back to Cu^{2+}.[3,4] Therefore, there is a need for quantitative knowledge of the processes leading to CuCl and $CuCl_2$ formation.

We previously reported a high-temperature fast-flow reactor (HTFFR) study of the reaction Cu + HCl, for which $k(680-1500\ K) = 1.2 \times 10^{-10}\exp(-7719\ K/T)$ cm^3 $molecule^{-1}$ s^{-1}. It was shown that this reaction in addition to CuCl + H leads to HCuCl,[7] which may further dissociate to CuCl + H. The subsequent oxidation of CuCl + HCl → $CuCl_2$ + H would be too endothermic, 176 kJ mol^{-1}, to be of practical interest. Here we extend the work to two additional reactions:

$$Cu(^2S) + Cl_2(X^1\Sigma) \rightarrow CuCl(X^1\Sigma) + Cl(^2P) \qquad \Delta_rH^\circ_{298} = -125 \pm 3\ kJ\ mol^{-1} \quad (1)$$

$$CuCl(X^1\Sigma) + Cl_2(X^1\Sigma) \rightarrow CuCl_2(X^2\Pi) + Cl(^2P) \qquad \Delta_rH^\circ_{298} = -13\ kJ\ mol^{-1} \quad (2)$$

These thermochemical data and spectroscopic notations are taken from the JANAF tables.[8] However, $\Delta_rH^\circ_{298}$ for $CuCl_2$ was obtained from Gurvich et al.,[9] who gave no uncertainty estimate; its state designation is from Churassy et al.[10]

The reaction

$$Cu(^2S) + N_2O(X^1\Sigma) \rightarrow CuO(X^2\Pi) + N_2(X^1\Sigma) \qquad \Delta_rH^\circ_{298} = -113 \pm 43\ kJ\ mol^{-1} \quad (3)$$

had previously been studied by our pseudostatic MHTP (metals high-temperature photochemistry) technique[11] and subsequently by Vinckier et al.[12] in a plasma afterglow fast-flow reactor. The latter led to somewhat lower rate coefficient values and a 15% increase in activation energy, which they noted is outside the experimental uncertainties. To investigate this discrepancy further, we have here included HTFFR measurements on this reaction.

Technique

The basic features and procedures of the HTFFR technique have been described previously.[13−16] A vertical reaction tube (2.2-cm i.d.) is surrounded and radiatively heated by SiC resistively heated rods inside an insulated water-cooled vacuum housing (Figure 1). For the study of reactions 1 and 3, a quartz reaction tube was used. Free Cu atoms were produced by the vaporization of Cu powder inside a resistively heated crucible and entrained by a Ar bath gas. Downstream from the Cu source, oxidant Ox/Ar mixtures are introduced through an axially movable ring inlet at 4 to 9% of the main Ar flow rate. The relative Cu concentrations were measured by laser-induced

* Corresponding author. E-mail: fontia@rpi.edu.
† Deceased.
‡ Present address: Argonne National Laboratory, Chemistry Division, Argonne, Illinois 60439-4831.

10.1021/jp030520r CCC: $25.00
Published on Web 10/08/2003

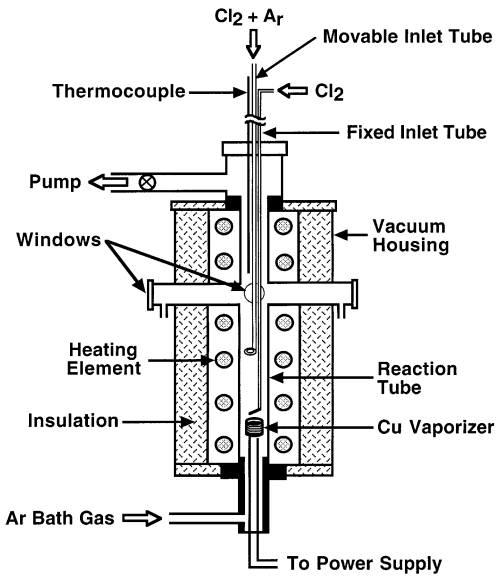

Figure 1. Schematics of the HTFFR reactor.

fluorescence (LIF) as a function of the reaction parameters. The laser system employed is a pulsed Lambda Physik EMG 101 excimer/FL 2002 dye laser in combination with a KDP doubling crystal. Fluorescence is generated using the Cu ($^2S_{1/2}$ to $^2P^0_{3/2}$) transition at 324.76 nm and observed through a 324.7-nm (2.5-nm full width at half-maximum) interference filter. The intensity of the fluorescence is measured by an EMI 9813QA photomultiplier tube, connected to a Data Precision Analogic 6000/620 100-MHz transient digitizer.

Rate coefficient measurements were made under pseudo-first-order conditions, [Cu] ≪ [Ox] ≪ [Ar], using the stationary inlet mode[15] with reaction-zone length distances set at 10 or 20 cm. Rate coefficients k_i for each temperature, pressure, and average velocity were obtained by using five different [Ox], providing variation by about a factor of 5. The maximum [Ox] used is given in the results tables below. k_i and σ_{k_i} were calculated by applying a weighted linear regression[17] to plots of $\ln[Cu]_{relative}$ versus [Ox]. These calculations yield straight lines with slopes equal to $-k_i t$, where t is the reaction time.

Mainly the same equipment and procedures are used for reaction 2. However, the quartz reaction tube was replaced by a mullite tube, which leads to reduced light scattering. A fixed Cl_2 inlet, located 1 cm downstream from the Cu vaporizer, was added to the apparatus. Through it, Cl_2 at concentrations of $(0.4-4.6) \times 10^{13}$ cm^{-3} flowed to convert Cu to CuCl. This was adequate to complete this conversion upstream from the movable Cl_2/Ar inlet. Separating the two reaction regimes imposed some limitations on the P, T, and flow-condition ranges over which reaction 2 could be studied. A second method for CuCl production was also used. There, CuCl was generated by passing mixtures of $CuCl_2$ vapor with Ar through a microwave discharge upstream from the HTFFR. Although the CuCl concentrations obtained from this source were much higher than when using Cu + Cl_2, the process was characterized by strong particle formation. The use of Cu_2Cl_2 instead of $CuCl_2$ was also investigated but was found to lead to even stronger particle formation. Therefore, it was not used for any measurements.

CuCl was positively identified by observing the following bands: 433.3 (0, 0), 425.9 (1, 0), and 418.9 nm (2, 0) from the $E^1\Sigma-X^1\Sigma$ system and 435.3 (0, 0) and 428.1 nm (1, 0) from the $D^1\Pi-X^1\Sigma$ system.[18] Only the strongest transition, 433.3 nm, was used for pumping and the detection of the LIF in the kinetic measurements. The fluorescence is observed through a 430-nm (23-nm fwhm) interference filter.

The materials used were Ar (99.998%) from the liquid (Praxair), 0.029% Cl_2 (99.5%) in Ar (99.995%), 0.334% Cl_2 (99.5%) in Ar (99.995%), Cl_2 (99.99%), 0.53% N_2O (99.99%) in Ar (99.998%), and N_2O (99.99%), all from Matheson, and 3.00% Cl_2 (99.9%) in Ar (99.995%) from Linde. Cu powder (99.5%, −40 + 100 mesh), Cu shot (99.9%, 1−10 mm), and $CuCl_2$ (99%, anhydrous) were obtained from Alfa Aesar. The Cl_2 flowed through Drierite ($CaSO_4$) drying towers.

Results and Discussion

Cu + Cl_2. Rate coefficients for reaction 1 are summarized in Table 1 and span the temperature range from 580−1140 K. The lower temperature limit was set by the heating effect of the vaporizer, and the upper limit, by the onset of Cl_2 dissociation.[19,20] The other reaction conditions including pressure and corresponding total concentration [M], maximum Cl_2 concentration $[Cl_2]_{max}$, observed reaction-zone length z, average velocity v, and laser intensity F were also varied; their values are listed in Table 1 together with the individual rate coefficients k_i that were measured. Residual analysis based on examination of $[k(T) - k_i]/k(T)$ plots versus the listed variables and absorption lines showed the rate coefficients to be independent of these. The measurements are shown in Arrhenius form in Figure 2. Also given there are the data points from the Vinckier et al.[21] study of reaction 1, which covered the 305−809 K temperature range. The two data sets show good agreement. They are combined and fitted by a weighted linear regression[22] of the form

$$k(T) = A \exp(-E\ \mathrm{K}/T) \qquad (4)$$

to yield

$$k_1(305 - 1140\ \mathrm{K}) = 3.89 \times 10^{-10} \times \exp(-355\ \mathrm{K}/T)\ \mathrm{cm^3\ molecule^{-1}\ s^{-1}} \qquad (5)$$

The variances and covariances[23] are $\sigma_A^2 = 5.73 \times 10^{-3}$ A^2, $\sigma_E^2 = 1.31 \times 10^3$, and $\sigma_{AE} = 2.53$ A. Using these to calculate the $\pm 2\sigma_k$ precision limits yields precision limits varying from 6 to 11% depending on temperature. Allowing for a ±10% uncertainty in the flow profile[13−15] and ±20% for other systematic errors yields $\pm 2\sigma_k$ confidence intervals of 23 to 25%.

A general mechanism for metal atom−Cl_2 reactions has previously been presented.[24] Briefly, because of the antibonding character of the interacting σ^* orbital of Cl_2, Cl_2 reactions can proceed only via mechanisms that involve bond breaking (i.e., abstraction or insertion). The metal-atom insertion into the Cl_2 bond would occur under C_{2v} symmetry. Because the interacting orbitals of Cu and Cl_2, 4s and σ^*, transform as a1 and b2 under C_{2v} symmetry, insertion would be symmetry-forbidden. In light of these arguments, the speculation by Sadeghi et al.[25] that the Cu + Cl_2 reaction proceeds via an insertion intermediate appears unlikely. Both the approximately gas kinetic magnitude of the rate coefficients and their pressure independence indicate abstraction as the reaction path (eq 1).

The large, nearly temperature-independent k values found in the present work are in accord with the exothermic metal atom−Cl_2 reactions (i.e., those of alkali metals,[26] Ca,[27] Sr,[27] Al,[20] Mg,[28] Pb,[29] Cr,[30] and Ti[31]). Most of those can be satisfactorily explained in terms of a harpooning or modified-harpooning mechanism. Vinckier et al. have shown that such models are inadequate for quantitatively describing the Cu[21] and Mg[28] reactions. They suggested that short-range charge-transfer

TABLE 1: Summary of Rate Coefficient Measurements on Cu + Cl_2

T, K	P, mbar	[M], 10^{17} cm^{-3}	$[Cl_2]_{max}$, 10^{11} cm^{-3}	v, m s^{-1}	reaction-zone length, cm	F, (arbitrary units)	$k_i \pm \sigma_{k_i}$ cm^3 molecule^{-1} s^{-1}
575	12.4	1.6	12.8	56	20	69	$(3.78 \pm 0.96) \times 10^{-10}$
588	42.0	5.2	20.8[a]	21	20	363	$(1.85 \pm 0.31) \times 10^{-10}$
636	42.1	4.8	28.5[a]	23	10	111	$(3.13 \pm 0.50) \times 10^{-10}$
725	29.5	2.9	18.2	29	20	279	$(3.15 \pm 0.54) \times 10^{-10}$
725	11.6	1.2	69.1[a]	88	10	57	$(3.94 \pm 1.07) \times 10^{-10}$
735	29.7	2.9	36.8	29	10	101	$(2.36 \pm 0.40) \times 10^{-10}$
737	17.4	1.7	35.2	36	10	67	$(3.36 \pm 0.71) \times 10^{-10}$
825	17.0	1.5	17.9[a]	40	20	56	$(2.81 \pm 0.60) \times 10^{-10}$
851	17.5	1.5	34.8	42	10	68	$(4.66 \pm 0.99) \times 10^{-10}$
874	17.5	1.4	39.9	42	10	76	$(2.85 \pm 0.60) \times 10^{-10}$
1037	51.0	3.6	9.6	22	20	144	$(2.21 \pm 0.33) \times 10^{-10}$
1039	59.1	4.1	11.0	19	20	99	$(3.03 \pm 0.47) \times 10^{-10}$
1109	59.5	3.9	10.4	20	10	157	$(2.55 \pm 0.38) \times 10^{-10}$
1140	80.6	5.1	13.7	15	20	212	$(2.55 \pm 0.39) \times 10^{-10}$

[a] Used 0.334% Cl_2 in Ar; otherwise, used 0.029% Cl_2 in Ar.

TABLE 2: Summary of Rate Coefficient Measurements on CuCl + Cl_2

T, K	P, mbar	[M], 10^{17} cm^{-3}	$[Cl_2]_{max}$, 10^{15} cm^{-3}	v, m s^{-1}	reaction-zone length, cm	F, (arbitrary units)	$k_i \pm \sigma_{k_i}$ cm^3 molecule^{-1} s^{-1}
984[a]	16.8	1.24	2.75	48	20	35	$(2.02 \pm 0.24) \times 10^{-13}$
997[a]	24.5	1.78	0.34[c]	32	10	147	$(3.03 \pm 0.27) \times 10^{-13}$
1024[a]	14.5	1.02	1.25	56	15	42	$(4.00 \pm 0.47) \times 10^{-13}$
1038[a]	20.5	1.43	1.20	58	20	29	$(3.06 \pm 0.35) \times 10^{-13}$
1053[a]	16.0	1.10	1.83	38	20	18	$(3.60 \pm 0.44) \times 10^{-13}$
1075[a]	13.1	0.88	1.59	44	15	28	$(2.53 \pm 0.32) \times 10^{-13}$
1098[a]	23.6	1.56	1.46	47	10	47	$(4.80 \pm 0.47) \times 10^{-13}$
1140[a]	21.3	1.36	1.61	63	10	46	$(4.77 \pm 0.50) \times 10^{-13}$
1142[a]	21.3	1.35	1.61	63	20	41	$(3.64 \pm 0.46) \times 10^{-13}$
1145[a]	23.2	1.47	0.28[c]	39	10	165	$(5.56 \pm 0.68) \times 10^{-13}$
1152[a]	12.2	0.77	0.24[c]	68	20	37	$(8.09 \pm 1.22) \times 10^{-13}$
979[b]	11.6	0.86	2.65	42	20	47	$(1.29 \pm 0.18) \times 10^{-13}$
999[b]	12.5	0.91	1.87	41	10	22	$(2.55 \pm 0.40) \times 10^{-13}$
1019[b]	14.4	1.02	1.83	41	10	34	$(1.44 \pm 0.19) \times 10^{-13}$
1059[b]	10.4	0.71	0.77	52	20	74	$(2.33 \pm 0.35) \times 10^{-13}$
1083[b]	13.7	0.92	1.37	43	20	34	$(2.92 \pm 0.43) \times 10^{-13}$
1086[b]	11.5	0.77	1.29	65	10	33	$(6.42 \pm 0.96) \times 10^{-13}$
1102[b]	19.7	1.30	0.88	45	10	27	$(8.30 \pm 0.77) \times 10^{-13}$
1130[b]	12.0	0.77	0.85	47	20	25	$(9.07 \pm 1.30) \times 10^{-13}$
1131[b]	15.2	0.97	1.03	39	20	48	$(6.36 \pm 0.77) \times 10^{-13}$
1138[b]	12.1	0.77	0.86	46	20	27	$(7.50 \pm 1.04) \times 10^{-13}$
1139[b]	13.0	0.83	1.76	43	10	23	$(4.42 \pm 0.62) \times 10^{-13}$

[a] CuCl produced by the Cu + Cl_2 reaction. [b] CuCl produced from $CuCl_2$. [c] Used 3.00% Cl_2 in Ar; otherwise, used pure (99.99%) Cl_2.

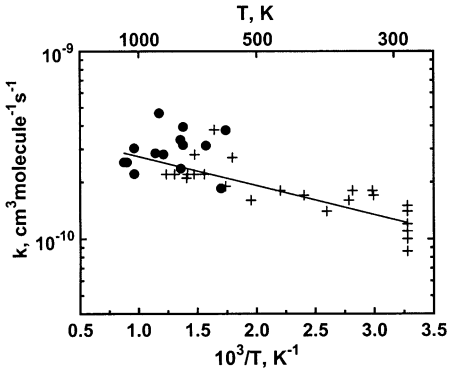

Figure 2. Summary of the Cu + Cl_2 rate coefficients. (●) Present HTFFR data. (+) Flow-tube data from ref 21. (—) Fit to the combined data, eq 5.

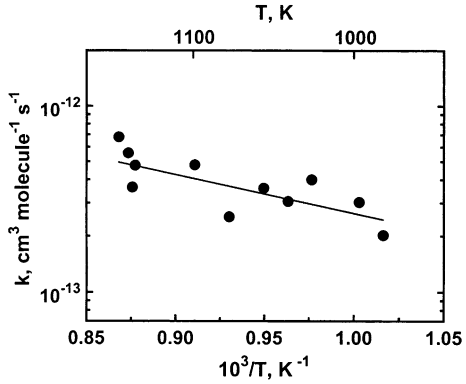

Figure 3. Arrhenius plot of the CuCl + Cl_2 rate coefficients.

interactions might be important. Campbell[31] found the harpoon model similarly inadequate for Ti. There thus appears to be no all-encompassing approach for describing metal atom−Cl_2 reactions, even though additional rate coefficient values can readily be predicted from the similarity of the many values already obtained.

CuCl + Cl_2. This reaction was investigated over the 980−1150 K temperature range and the 12−25 mbar pressure range. The upper temperature limit was again due to Cl_2 dissociation. The other restrictions were due to an increase in scattered laser radiation, attributed to particle formation. The results are summarized in the top part of Table 2 and in Figure 3. Residual analysis plots showed the data to be independent of the indicated parameters, except T. Such plots also indicate the rate coef-

TABLE 3: Summary of Rate Coefficient Measurements on Cu + N_2O

T, K	P, mbar	[M], 10^{17} cm^{-3}	$[N_2O]_{max}$, 10^{14} cm^{-3}	v, m s^{-1}	reaction-zone length, cm	F, (arbitrary units)	$k_i \pm \sigma_{k_i}$ cm^3 molecule^{-1} s^{-1}
529	47.9	6.6	244.0	13	10	83	$(1.03 \pm 0.15) \times 10^{-14}$
544	48.2	6.4	166.1	14	20	91	$(1.77 \pm 0.28) \times 10^{-14}$
583	13.2	1.6	77.1	42	20	68	$(3.31 \pm 0.80) \times 10^{-14}$
606	28.5	3.4	94.5	17	20	93	$(4.90 \pm 0.87) \times 10^{-14}$
609	28.7	3.4	94.4	17	10	85	$(4.06 \pm 0.69) \times 10^{-14}$
654	15.1	1.7	63.2	57	20	160	$(1.12 \pm 0.25) \times 10^{-13}$
682	13.7	1.5	26.7	36	10	34	$(1.92 \pm 0.46) \times 10^{-13}$
692	22.5	2.4	36.6	26	20	106	$(1.24 \pm 0.23) \times 10^{-13}$
700	13.7	1.4	21.4	37	20	52	$(2.01 \pm 0.48) \times 10^{-13}$
710	74.5	7.6	2.2[a]	11	20	53	$(2.45 \pm 0.35) \times 10^{-13}$
719	14.7	1.5	43.8	52	20	74	$(2.32 \pm 0.54) \times 10^{-13}$
775	12.3	1.2	23.8	68	20	86	$(4.14 \pm 1.08) \times 10^{-13}$
812	12.4	1.1	45.7	72	10	66	$(4.40 \pm 1.14) \times 10^{-13}$
828	10.0	0.9	21.1	93	20	114	$(4.73 \pm 1.42) \times 10^{-13}$
876	27.6	2.3	0.8[a]	18	20	146	$(8.81 \pm 1.45) \times 10^{-13}$
896	10.1	0.8	31.7	103	10	312	$(7.02 \pm 2.10) \times 10^{-13}$
949	13.7	1.0	15.1	86	20	174	$(9.23 \pm 2.22) \times 10^{-13}$

[a] Used 0.53% N_2O in Ar; otherwise, used pure (99.99%) N_2O.

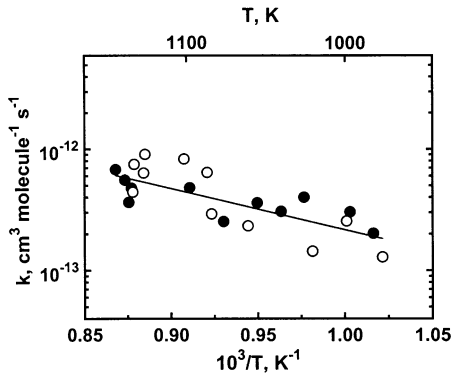

Figure 4. Comparison of CuCl + Cl_2 rate coefficients from two different CuCl sources. (●) CuCl from Cu + Cl_2. (○) CuCl from $CuCl_2$.

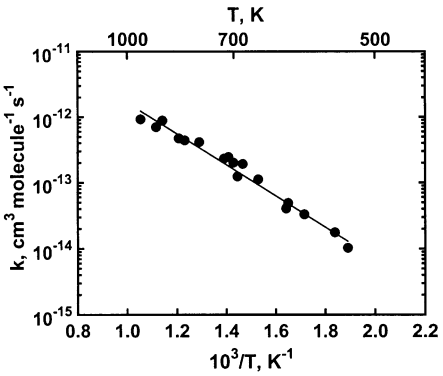

Figure 5. Summary of the Cu + N_2O rate coefficients. (●) Present study. (—) Fit to the present measurements, eq 8.

ficients to be independent of the scattered light intensities. The data were again fitted to eq 4 to yield

$$k_2(980 - 1150\ \mathrm{K}) = 3.10 \times 10^{-11} \times \exp(-4765\ \mathrm{K}/T)\ \mathrm{cm^3\,molecule^{-1}\,s^{-1}} \quad (6)$$

The calculated variances and covariance are $\sigma_A^2 = 3.3 \times 10^{-1}$ A^2, $\sigma_E^2 = 9.2 \times 10^5$, and $\sigma_{AE} = 3.1 \times 10^2$ A, which lead to $\pm 2\sigma_k$ precision limits of 38% at 980 K and 35% at 1150 K and corresponding accuracy limits of 44 and 41%.

Experiments using CuCl from $CuCl_2$ led to essentially the same k values (cf. the lower part of Table 2 and Figure 4). However, residual plots as a function of the scattered-light intensity showed the data to correlate somewhat with this quantity. These data are therefore not included in the recommended fitting expression. Their inclusion would have yielded $k_2(980-1150\ \mathrm{K}) = 5.3 \times 10^{-10} \exp(-7813\ \mathrm{K}/T)$ cm^3 molecule^{-1} s^{-1}.

Apparently, the only other metalmonohalide−Cl_2 reaction for which $k(T)$ values have been measured is[20]

$$\mathrm{AlCl + Cl_2 \rightarrow AlCl_2 + Cl} \qquad \Delta_r H^\circ_{298} = -108 \pm 21\ \mathrm{kJ\,mol^{-1}} \quad (7)$$

for which $k_7(400-1025\ \mathrm{K}) = 9.6 \times 10^{-11} \exp(-610\ \mathrm{K}/T)$ cm^3 molecule^{-1} s^{-1} was obtained. The small activation energy of 5.0 kJ mol^{-1} resembles that of the aforementioned exothermic metal atom−Cl_2 reactions. CuCl + Cl_2 exhibits a significantly larger activation energy, $E_a = 40$ kJ mol^{-1}. Because there is no estimate available for the uncertainty in the heat of formation of $CuCl_2$,[9] a thermal barrier in reaction 2 cannot a priori be excluded. However, the high E_a of the CuCl + Cl_2 reaction is likely due to the closed-shell structure of CuCl. To accommodate the second Cu−Cl bond, the Cu atom has to undergo a $3d^{10}4s^1 \rightarrow 3d^94s^2$ promotion and a subsequent 4s−4p hybridization. Several CuCl excited states that correlate with the $3d^94s^2$ state are known.[32] Their excitation energies (≥227 kJ mol^{-1}) exceed the measured activation energy, whose barrier is apparently lowered because of the influence of the incoming Cl atom. AlCl, which has an open p-shell structure, does not require an additional promotion for the 3s−3p hybridization to occur.

Cu + N_2O. The measured values of the rate coefficients and the conditions under which they were obtained are given in Table 3. Residual plots show the data to be independent of parameters other than temperature. The fit of the data to eq 4 is shown in Figure 5 and is given by

$$k_3(530 - 950\ \mathrm{K}) = 3.80 \times 10^{-10} \times \exp(-5441\ \mathrm{K}/T)\ \mathrm{cm^3\,molecule^{-1}\,s^{-1}} \quad (8)$$

with $\sigma_A^2 = 1.31 \times 10^{-1}$ A^2, $\sigma_E^2 = 6.15 \times 10^4$, and $\sigma_{AE} = 8.83 \times 10^2$ A. These yield $\pm 2\sigma_k$ precision limits varying from 13 to 26% depending on temperature. Using the same systematic errors as above results in confidence intervals varying from ±26 to ±34%.

In Figure 6, the present results are compared to those of our previous pseudostatic photochemical study of this reaction, which covered the 470−1340 K range,[11] and to Vinckiers'[12]

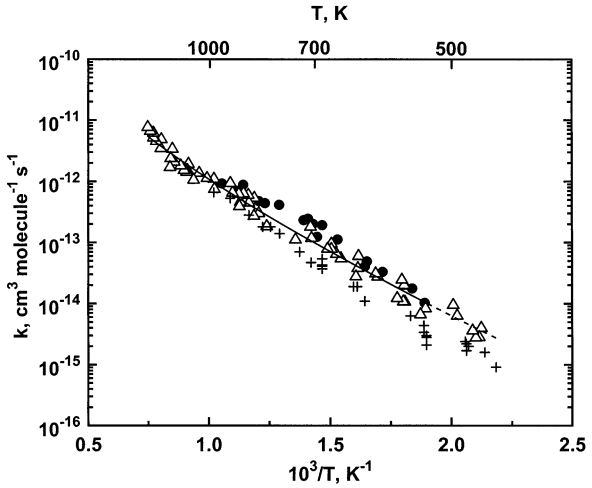

Figure 6. Comparison of the rate coefficient measurements for the Cu + N_2O reaction. (●) Present HTFFR data. (△) Data from the MHTP study, ref 11. (+) Flow-tube data from ref 12. (—) Fit of combined measurements, eq 10. (- - -) Extension of the eq 10 fit.

fast-flow reactor measurements from 458 to 980 K. The methods of the latter differ from those of the present work in the Cu-atom production (plasma-vaporized Cu_XCl_Y reaction with H atoms) and detection (atomic absorption spectroscopy) methods. However, the basic phenomenology and analysis is similar to that of the present work. The HTFFR and MHTP measurements well agree in the main temperature range (as was also found in a previous metal-atom oxidation study),[30] but the HTFFR data are somewhat higher at midrange temperatures. The Vinckier data are somewhat lower than those from the MHTP work, but at least at $T \geq 530$ K the three sets can readily be combined and fitted to the nonlinear expression

$$k(T) = AT^n \exp(-E\ \mathrm{K}/T) \qquad (9)$$

which yields

$$k_3(530 - 1340\ \mathrm{K}) = 2.85 \times 10^{-19} (T/\mathrm{K})^{2.67} \times \exp(-3291\ \mathrm{K}/T)\ \mathrm{cm^3\,molecule^{-1}\,s^{-1}} \qquad (10)$$

with variances and covariances of $\sigma_A^2 = 1.13 \times 10^1$ A^2, $\sigma_n^2 = 1.90 \times 10^{-1}$, $\sigma_E^2 = 1.20 \times 10^5$, $\sigma_{An} = -1.47$ A, $\sigma_{nE} = -1.50 \times 10^2$, and $\sigma_{AE} = 1.16 \times 10^3$ A. The resulting $\pm 2\sigma_k$ precision limits vary from a minimum of 4% at 1050 K to a maximum of 13% at 470 K, with corresponding confidence intervals of ± 23 to ± 26%.

This best-fit line is shown in Figure 6. Its extension to lower temperatures fits the MHTP data in that range very well, but the more scattered Vinckier data are decidedly lower. It should be noted that the latter results are in the (0.9 to 3) $\times 10^{-15}$ range, which is close to the limit of detection of fast-flow tube techniques and thus are less reliable. Without these data, their activation energy would decrease and approximate more closely those from the MHTP observations. We thus conclude that there is no significant difference between the results from Vinckier and our laboratory (as is also the case for the Cu + Cl_2 measurements discussed above). Our previous recommendation[11] of

$$k_3(470 - 1340\ \mathrm{K}) = 3.04 \times 10^{-20} (T/\mathrm{K})^{2.97} \times \exp(-3087\ \mathrm{K}/T)\ \mathrm{cm^3\,molecule^{-1}\,s^{-1}} \qquad (11)$$

thus does not need to be adjusted. Equations 10 and 11 agree within 10% over the whole temperature range.

Acknowledgment. This work was supported under NSF grants CTS-0224778 and CTS-9905265, Dr. Farley Fisher, Program Director. We thank W. F. Flaherty, T. Radosavljevic, and B. Banovic for assistance.

References and Notes

(1) Jay, K.; Stieglitz, L. *Chemosphere* **1991**, *22*, 987.
(2) Addink, R.; Olie, K. *Environ. Sci. Technol*. **1995**, *29*, 1425.
(3) Stieglitz, L. *Environ. Eng. Sci*. **1998**, *15*, 5.
(4) Weber, P.; Dinjus, E.; Stieglitz, L. *Chemosphere* **2001**, *42*, 579.
(5) Addink, R.; Altwicker, E. R. *Environ. Eng. Sci*. **1998**, *15*, 19.
(6) Taylor, P. H.; Sidhu, S. S.; Rubey, W. A.; Dellinger, B.; Wehrmeir, A.; Lenoir, D.; Schramm, K.-W. *Proc. Comb. Inst*. **1998**, *27*, 1769.
(7) Belyung, D. P.; Hranisavljevic, J.; Kashireninov, O. E.; Santana, G. M.; Fontijn, A.; Marshall, P. *J. Phys. Chem*. **1996**, *100*, 17835.
(8) Chase, M. W., Jr. NIST-JANAF Thermochemical Tables; *J. Phys. Chem. Ref. Data* **1998**, Monograph 9.
(9) Gurvich, L. V.; Iorish, V. S.; Yungman, V. S.; Dorofeeva, O. V. In *Handbook of Chemistry and Physics*, 82nd ed.; Lide, D. R., Ed.; Wiley and Sons: New York, 2001; p 5—73.
(10) Churassy, S.; Koffend, J. B.; Crozet, S.; Russier, I. *J. Phys. Chem*. **1994**, *98*, 7991.
(11) Narayan, A. S.; Futerko, P. M.; Fontijn, A. *J. Phys. Chem*. **1992**, *96*, 290.
(12) Vinckier, C.; Verhaeghe, T.; Vanhees, I. *J. Chem. Soc., Faraday Trans*. **1994**, *90*, 2003.
(13) Fontijn, A.; Futerko, P. M. In *Gas-Phase Metal Reactions*; Fontijn, A., Ed.; North-Holland: Amsterdam, 1992; Chapter 6.
(14) Slavejkov, A. G.; Futerko, P. M.; Fontijn, A. *Proc. Comb. Inst.* **1990**, *23*, 155.
(15) Fontijn, A.; Felder, W. In *Reactive Intermediates in the Gas Phase: Generation and Monitoring*; Setser, D. W., Ed.; Academic Press: New York, 1979; Chapter 2.
(16) Fontijn, A. *Pure Appl. Chem.* **1998**, *70*, 469.
(17) Irvin, J. A.; Quickenden, I. T. *J. Chem. Educ.* **1983**, *60*, 711.
(18) Pearse, R. W. B.; Gaydon, A. G. *The Identification of Molecular Spectra*, 4th ed.; Chapman and Hall: London, 1976; p 148.
(19) Slavejkov, A. G.; Stanton, C. T.; Fontijn, A. *J. Phys. Chem*. **1990**, *94*, 3347.
(20) Rogowski, D. F.; Marshall, P.; Fontijn, A. *J. Phys. Chem*. **1989**, *93*, 1118.
(21) Vinckier, C.; Verhaeghe, T.; Vanhees, I. *J. Chem. Soc., Faraday Trans*. **1996**, *92*, 1445.
(22) Press, W. H.; Flannery, B. P.; Teukolsky, S. A.; Vetterling, W. T. *Numerical Recipes*; Cambridge University Press: Cambridge, U.K., 1986; Chapter 14.
(23) Wentworth, W. E. *J. Chem. Educ*. **1965**, *42*, 96, 162.
(24) Hranisavljevic, J.; Fontijn, A. *J. Phys. Chem. A* **1997**, *101*, 2323.
(25) Sadeghi, I.; Hikmet, I.; Colomb, I.; Setser, D. W.; In *Gas-Phase Metal Reactions*; Fontijn, A., Ed.; North-Holland: Amsterdam, 1992; Chapter 18.
(26) Husain, D. *J. Chem. Soc., Faraday Trans. 2* **1989**, *85*, 85.
(27) Vinckier, C.; Helaers, J.; Remeysen, J. *J. Phys. Chem. A* **2000**, *104*, 6406.
(28) Vinckier, C.; Christiaens, P. *J. Phys. Chem*. **1992**, *96*, 8423.
(29) Cosic, B.; Fontijn, A. *J. Phys. Chem. A* **2000**, *104*, 5517.
(30) Fontijn, A.; Blue, A. S.; Narayan, A. S.; Bajaj, P. N. *Combust. Sci. Technol*. **1994**, *101*, 59.
(31) Campbell, M. L. *J. Phys. Chem*. **1993**, *97*, 3922.
(32) Guichemerre, M.; Ghambaud, G.; Stoll, H. *Chem. Phys*. **2002**, *280*, 71.